

# In vitro corrosion behaviour of Mg alloys in a phosphate buffered solution for bone implant application

Liping Xu · Erlin Zhang · Dongsong Yin ·  
Songyan Zeng · Ke Yang

Received: 24 July 2006 / Accepted: 10 January 2007 / Published online: 1 August 2007  
© Springer Science+Business Media, LLC 2007

**Abstract** The corrosion behaviour of Mg–Mn and Mg–Mn–Zn magnesium alloy in a phosphate buffered simulated body fluid (SBF) has been investigated by electrochemical testing and weight loss experiment for bone implant application. Long passivation stage and noble breakdown potential in the polarization curves indicated that a passive layer could be rapidly formed on the surface of magnesium alloy in the phosphate buffered SBF, which in turn can protect magnesium from fast corrosion. Surfaces of the immersed magnesium alloy were characterized by SEM, EDS, SAXS and XPS. Results have shown that Mg–Mn and Mg–Mn–Zn alloy were covered completely by an amorphous Mg-containing phosphate reaction layer after 24 h immersion. The corrosion behaviour of magnesium alloys can be described by the dissolving of magnesium through the reaction between magnesium and solution and the precipitating of Mg-containing phosphate on the magnesium surface. Weight loss rate and weight gain rate results have indicated that magnesium alloys were corroded seriously at the first 48 h while Mg-containing phosphate precipitated fast on the surface of magnesium alloy. After 48–96 h immersion, the corrosion reaction and the precipitation reaction reach a stable stage, displaying that the phosphate layer on magnesium surface, especially Zn-containing phosphate layer could provide effective protection for magnesium alloy.

## Introduction

Magnesium alloys have shown much potential for bone implants due to their good biocompatibility, biodegradability or bioabsorbability, high strength compared to polymers and high ductility compared to bioceramics. The closer mechanical properties of magnesium alloys to natural bone than those of other metallic materials could significantly reduce the “stress shielding” existed in the metallic bone implants. Furthermore, the biodegradability provides the possibility to resolve the bone/implant interface problem, such as interface loose and inflammation. In addition, due to their biodegradability or bioabsorbability, the second surgery for removal of the metal bone plates and screws is not necessary in the case of magnesium implant. However, the high corrosion rate of magnesium and its alloys which results in the subcutaneous gas bubbles [1, 2] limits their clinical application. For example, it was reported some magnesium implants was corroded completely after 3–5 weeks [3] or 4–6 weeks postoperation [4]. Therefore, the main research activities are focused on how to increase the strength of magnesium alloy and protect magnesium from fast corrosion.

As well known, the corrosion of metal materials is mainly dependent on their composition. High purity magnesium alloy, such as 99.9999% Mg (or 6 N Mg) has shown good corrosion resistance [5]. Also it has been reported that the addition of Al element can increase the corrosion resistance against NaCl because of the formation of  $\text{Al}_2\text{O}_3$  surface layer [6]. Several magnesium alloys have been investigated for the bone implants materials, including AZ31, AZ91, AM60 and LAE442 [1, 5, 7–9]. However, previous studies on titanium alloy have shown that aluminium element could cause metal allergy [10]. It has been reported that WE43 alloy shows the best corrosion

---

L. Xu · E. Zhang (✉) · K. Yang  
Institute of Metal Research, Chinese Academy of Sciences,  
Shenyang 110016, China  
e-mail: erlin.zhang@imr.ac.cn

D. Yin · S. Zeng  
School of Materials Science and Engineering, Harbin Institute of  
Technology, Harbin 150001, China

resistance among the commercial available magnesium alloys due to the addition of yttrium [11]. Due to its good corrosion resistance, WE43 alloy has been implanted into rats to study the *in vivo* corrosion behaviour and bone response [1, 12]. However, no research results have been reported on the beneficial effect of Nd and Y rare earth elements on the bone health. On the contrary, Nd is not allowed to be used in make-up in China.

Manganese (Mn) has no toxic effect except after extreme occupational exposure. The highest concentrations of manganese are found in the bones, liver and pancreas [13]. Mn is an essential element and plays a primary role in the activation of multiple enzyme systems, i.e. hydrolases, kinases, transferases and mitochondrial respiration [14]. The recommended daily amount of Mn for ages 11–51 + is 2–5 mg [13]. Zinc is also an essential component of over 200 enzymes in the body, including RNA and DNA polymerases [15–17]. Zinc therefore contributes, via enzymes, a catalytic role, a regulatory role, e.g. in controlling and coordinating cell growth, and a structural role, e.g. as zinc finger proteins in body hormones [13, 16, 18].

Manganese (Mn) does not have much effect on tensile strength, but it does improve the saltwater resistance of magnesium alloy by removing iron and other heavy metal elements into relatively harmless intermetallic compounds, some of which will be separated out during melting [19]. Zinc (Zn) is next to aluminium in effectiveness as an alloying element in magnesium to improve room-temperature strength in combination with aluminium. Zinc also helps overcome the harmful corrosive effect of iron and nickel impurities.

In this paper, it is proposed that the addition of Mn and Zn could improve the corrosion resistance as well as the mechanical properties. Mg–Mn and Mg–Mn–Zn alloys were prepared and the corrosion behaviours were investigated *in-vitro* for the purpose of producing magnesium alloy with good corrosion properties and non-toxicity for bone implant materials by the addition of Mn and Zn alloy.

## Experimental

### Preparation of samples and solution

High purity Mg–Mn (Mg-1.2Mn, in wt%), Mg–Mn–Zn (Mg-1.2Mn-1.0Zn, in wt%) and WE43 (Mg-4.0Y-3.0Nd-0.5Zr, in wt%) were prepared in our laboratory. All specimens were cut from the magnesium alloys cast ingots. Samples for the electrochemical test and the immersion test were moulded into epoxy resin with only one side of 1 cm<sup>2</sup> exposed. The sample surfaces were ground with SiC emery papers of 400, 600, 800, 1000 and 2000 grits, and finely polished with 0.5 μm diamond powders, then ultrasonically

cleaned in alcohol for 5 min and dried in air. Simulated body fluid (SBF) was used as corrosion medium. The chemical composition of SBF solution was listed in Table 1. Phosphates (KH<sub>2</sub>PO<sub>4</sub> and Na<sub>2</sub>HPO<sub>4</sub>) were used as buffer in order to keep the pH value in a range of 7.3–7.5 during experiments. Before tests, the pH of the SBF solution was adjusted to 7.3 by addition of NaOH.

### Electrochemical test

Electrochemical tests were carried out at 37 °C ± 1 °C in the solution using an automatic laboratory corrosion measurement system. The tests were carried out in a beaker containing 350 mL solution using a standard three-electrode configuration, the saturated calomel as a reference, a platinum electrode as the counter and the sample as the working electrode. The open circuit potential ( $E_{ocp}$ ) was measured as a function of time. In the potentiodynamic polarization tests, firstly the working electrode was immersed in the solution for 20 min and then the polarization curve was measured at a scanning rate of 0.3 mV/s.

### Weight gain/loss test

Samples were immersed in a 500 mL solution (total surface area to solution volume = 1 cm<sup>2</sup>:500 mL) at 37 °C ± 1 °C for 24, 48, 96 and 216 h, respectively. Then the samples were supersonically washed in distilled water. The sample weight was measured before and after the immersion by a balance with an accuracy of 0.1 mg to calculate the weight gain (weight gain = (weight after immersion–weight before immersion)/surface area). The immersed samples were cleaned using a boiling solution of 180 g/L chromic acid to remove the surface corrosion product, and then rinsed with ethanol, dried in air and finally weighted to calculate the weight loss (weight loss = (weight before immersion–weight after clean)/surface area).

### Microstructure

After being washed supersonically in distilled water, the surface morphologies of the immersed samples were observed on a SSX-550 scanning electronic microscopy (SEM). The chemical composition of the surface layer or products was determined by energy dispersive spectroscopy (EDS). Surface structure of the immersed samples

**Table 1** Chemical composition of SBF solution (g/L)

NaCl	Na <sub>2</sub> HPO <sub>4</sub>	NaHCO <sub>3</sub>	KCl	KH <sub>2</sub> PO <sub>4</sub>	MgSiO <sub>4</sub> · 7H <sub>2</sub> O	CaCl <sub>2</sub>
8.0	0.06	0.35	0.4	0.06	0.2	0.14

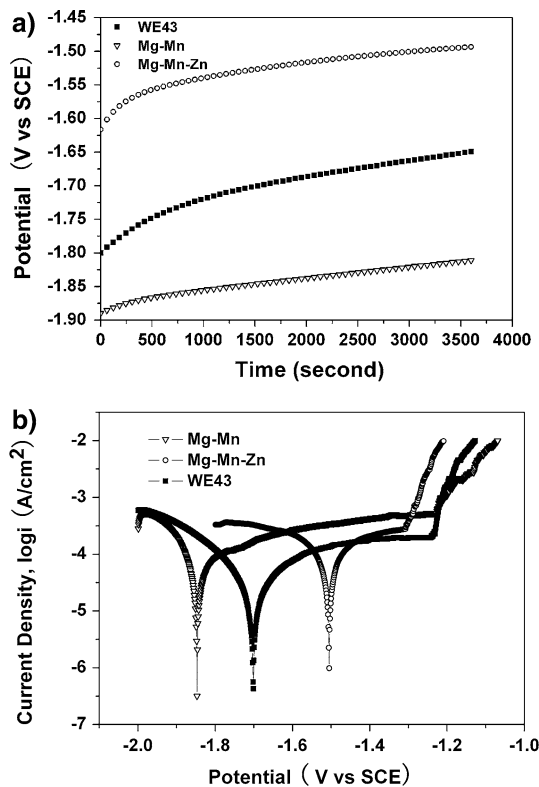


**Fig. 1** (a) The open circuit potential against immersion time and (b) the electrochemical polarization curves of magnesium alloys in phosphate buffered solution

was characterized by X-ray photoelectron spectroscopy (XPS, Escalab250, Thermo Corp.). The XPS measurements were performed using an X-ray source of Mg Ka (1253.6 eV). Measured binding energies were corrected by referring the binding energy of C<sub>1s</sub> of methylene groups of the hydrocarbon (284.6 eV) adsorbed on the surface of substrate. In order to identify the phase constituents of the surface reaction product on the magnesium samples immersed for 216 h, the surface was examined with small angle X-ray scattering (SAXS) which was conducted on a X-ray diffractometer (XRD, D/MAX-RB, Rigaku) with an incident angle of 2 degree against surface of the specimens, and the measurements were performed with a continuous scanning mode at a rate of 4°/min.

## Results

### Electrochemical testing

Open circuit potential (OCP) curves and polarization curves of three alloys are shown in Fig. 1a and b, respectively. The highest  $E_{ocp}$  is found for Mg–Mn–Zn alloy and the lowest  $E_{ocp}$  for Mg–Mn alloy. In the polarization curves, a long passivation stage and noble breakdown potential can be observed at the anodic polarization stage for all alloys, as shown in Fig.1b. The electrochemical parameters obtained from Fig. 1 are listed in Table 2. The corrosion potentials ( $E_{corr}$ ) increases in the order of  $E_{corr}(\text{Mg–Mn}) < E_{corr}(\text{WE43}) < E_{corr}(\text{Mg–Mn–Zn})$ . Although the corrosion current densities ( $i_{corr}$ ) of three alloys are of the same order of magnitude, WE43 alloy shows the lowest  $i_{corr}$ , only one fifth that of Mg–Mn and Mg–Mn–Zn alloys, indicating that WE has better corrosion resistance than other two alloys.

### Weight gain and surface morphology

Figure 2 shows the weight gain and the surface morphology of Mg–Mn at different immersion time. About 4 mg/cm<sup>2</sup> weight gain is observed after 24 h immersion and the weight gain increases with the increase of the immersion time. After 216 h immersion, about 15.0 mg/cm<sup>2</sup> weight is gained. Microstructure observation shows that the magnesium surface is completely covered after 24 h immersion by a reaction layer with many cracks on the surface. EDS analysis was conducted on several small surface areas and the result is shown in Fig. 3. The element quantitative analysis results are listed in Table 3. The result indicates that this layer is mainly composed of O, P, Mg, Na and Ca, small amount of K, and tiny amount of Mn, as listed in Table 3. A high Mg content is found in this layer. Ca/P is only about 0.17, much less than that of hydroxyapatite. However, a high Mg/Ca of 5.21 is found in this layer. With increase of the immersion time, for example, after 96 h immersion, there is slightly difference in the surface morphology and some small particles are formed in the reaction layer. No significant difference is found in the element analysis results by EDS.

**Table 2** Electrochemical data of magnesium alloys in phosphate buffered SBF solution

Alloys	OCP(60min) V	Rp ohm	$i_{corr}$ , A/cm <sup>2</sup>	$E_{corr}$ , V	Eb, V	$\Delta E(Eb-E_{corr})$ V
Mg–Mn	–1.810	382	$5.656 \times 10^{-5}$	–1.847	–1.227	0.620
Mg–Mn–Zn	–1.494	233	$7.917 \times 10^{-5}$	–1.505	–1.308	0.197
WE43	–1.644	1234	$1.603 \times 10^{-5}$	–1.701	–1.241	0.460

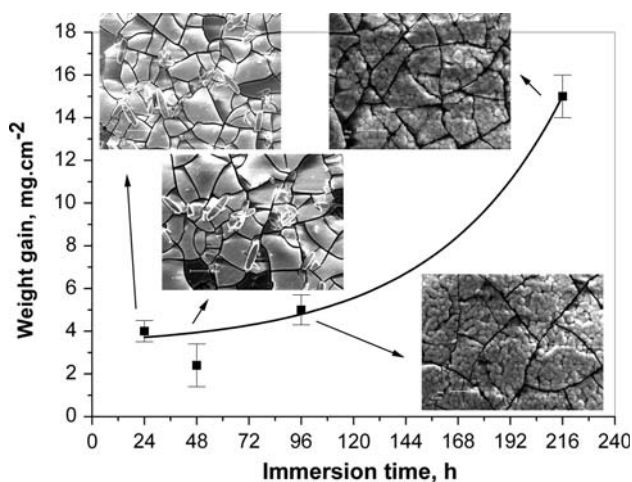


**Fig. 2** Weight gain and morphology of Mg–Mn alloy in the phosphate buffered SBF solution

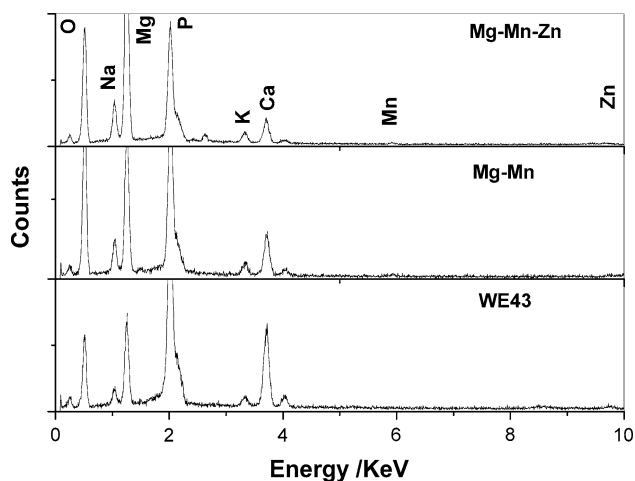


**Fig. 3** EDS analysis results on the surface of magnesium alloy after 24 h immersion. EDS analysis was conducted on a small area on the surface of Mg–Mn and Mg–Mn–Zn alloys, and on the reaction product of WE43

In order to identify the phase constitute of this reaction layer, a small angle X-ray scanning (SAXS) was conducted on the magnesium surface, which had been immersed for

216 h, as shown in Fig. 4. A large amount of amorphous phase as well as magnesium matrix can be detected in this reaction layer. Figure 5 shows  $P_{2p}$ ,  $Ca_{2p}$ ,  $O_{1s}$ ,  $Mg_{1s}$  and  $Mn_{2p}$  XPS spectra of the surface of Mg–Mn, which has been immersed for 216 h. It can be seen from Fig. 5 that  $P_{2p_{3/2}}$  spectrum is detected as single speak at 132.9 eV and  $Ca_{2p}$  spectra are detected as doublet peaks of  $Ca_{2p_{3/2}}$  at 347.6 eV and  $Ca_{2p_{1/2}}$  at 350.7 eV. From the bonding energies of  $P_{2p_{3/2}}$  and  $Ca_{2p}$ , it can be concluded that P element exists in the layer in a form of phosphate group.  $O_{1s}$  and  $Mg_{1s}$  spectra are detected as single peak at 531.2 eV and 1304.1 eV, respectively. Small amount of Mn is also detected by XPS.  $Mn_{2p}$  spectra are detected as doublet peaks of  $Mn_{2p_{3/2}}$  at 641.9 eV and  $Mn_{2p_{1/2}}$  at 654.2 eV, displaying that Mn exists in a form of MnO. Combined with the SAXS result shown in Fig. 4, it can be concluded that the surface reaction layer is mainly a kind of amorphous Mg-containing phosphate layer with small amount of MnO.

For Mg–Mn–Zn alloy, Fig. 6, a similar tendency is present in the weight gain against immersion time except that the weight gain of Mg–Mn–Zn alloy is lower than that of Mg–Mn alloy. For example, 9.7 mg/cm<sup>2</sup> weight is gained after 216 h immersion. Morphology observation shows that the surface is also completely covered by a reaction layer after 24 h immersion as it did in the case of Mg–Mn alloy. EDS analysis results which were conducted on several small areas indicate that the reaction layer is also composed of O, P, Mg, Na and Ca, small amount of K, and tiny amount of Mn and Zn, as shown in Fig. 3 and Table 3. Ca/P is about 0.20 and Mg/Ca is about 8.10. Large amount of amorphous phase as well as small amount of  $Ca_{10}Na(PO_4)_7$  are identified by SAXS, as shown in Fig. 4. Figure 7 shows  $P_{2p}$ ,  $Ca_{2p}$ ,  $O_{1s}$ ,  $Mg_{1s}$ ,  $Mn_{2p}$  and  $Zn_{2p}$  XPS spectra of the surface of Mg–Mn–Zn which has been immersed for 216 h. Small amount of Zn is detected by XPS as doublet peaks of  $Zn_{2p_{3/2}}$  at 1022.8 eV and  $Zn_{2p_{1/2}}$  at 1045.7 eV. However, it is difficult to identify the exact existing form of Zn from the XPS results. From the XPS and SAXS results, it can be confirmed that the surface reaction layer is also mainly a kind amorphous Mg-containing phosphate layer with small amount of MnO.

**Table 3** EDS analysis results on the surface reaction layer of Mg–Mn and Mg–Mn–Zn alloys and the surface reaction products of WE43 alloy immersed for 24 h

Alloys	Element percent (at. %)								Ca/P	Mg/Ca
	O	Na	Mg	P	K	Ca	Mn	Zn		
Mg–Mn	75.48 ± 2.05	3.07 ± 3.62	8.47 ± 0.10	9.83 ± 0.68	1.26 ± 0.79	1.62 ± 0.01	0.28 ± 0.01	–	0.17 ± 0.01	5.21 ± 0.08
Mg–Mn–Zn	67.62 ± 0.97	3.47 ± 0.03	15.82 ± 1.14	10.20 ± 1.14	0.63 ± 0.06	2.02 ± 0.46	0.21 ± 0.08	0.051 ± 0.02	0.20 ± 0.07	8.10 ± 2.42
WE43	70.12 ± 0.59	1.14 ± 0.53	7.98 ± 2.57	14.86 ± 1.56	0.92 ± 0.19	4.69 ± 0.65	–	–	0.31 ± 0.01	1.76 ± 0.79

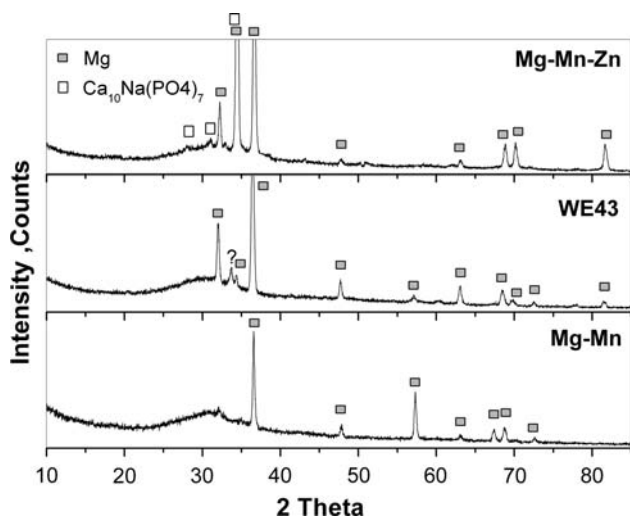


**Fig. 4** SAXS diffraction patterns of the surfaces of Mg alloys after 216 h immersion in phosphate buffered SBF solution

Figure 8 shows the weight gain of WE43 alloy against immersion time. WE43 alloy also shows a similar tendency in the weight gain against immersion time to Mg–Mn and Mg–Mn–Zn alloys, and the weight gain of WE43 after 216 h immersion is about 11.7 mg/cm<sup>2</sup>, less than that of Mg–Mn and slightly higher than that of Mg–Mn–Zn alloys. On the surface, only small amount of reaction products rather than a complete reaction layer is observed even after 96 h immersion while the second phase in WE43 is clearly observed. EDS results conducted on the reaction products indicates that the reaction products are mainly composed of O, P, Mg, Na and Ca, and small amount of K, similar to the

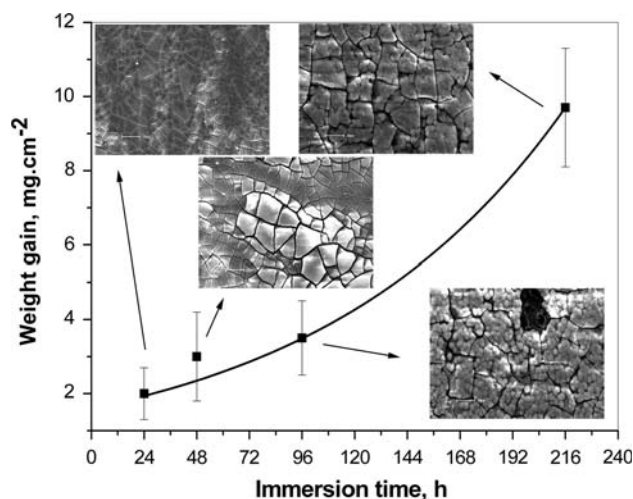


**Fig. 6** Weight gain and morphology of Mg–Mn–Zn alloy in the phosphate buffered SBF solution

reaction layers formed on the surface of Mg–Mn and Mg–Mn–Zn alloy. Ca/P is about 0.31, slightly higher than those of the reaction layers. Only amorphous phase is identified by SAXS on the surface of WE 43 alloy immersed for 216 h, as shown in Fig. 4. Figure 9 shows P<sub>2p</sub>, Ca<sub>2p</sub>, O<sub>1s</sub>, Mg<sub>1s</sub> and Y<sub>3d</sub> XPS spectra of the surface of WE43 alloy which has been immersed for 216 h. Slight shift of P<sub>2p</sub> and Ca<sub>2p</sub> spectra is observed compared with that observed on the surface of Mg–Mn and Mg–Mn–Zn alloy, but the bonding energy data still demonstrate that P exists in a form of phosphate. Y<sub>3d5/2</sub> spectra are detected as a single peak at 158.6 eV. However, no Nd spectra are detected by XPS on the surface.

**Fig. 5** P<sub>2p</sub>, Ca<sub>2p</sub>, O<sub>1s</sub>, Mg<sub>1s</sub> and Mn<sub>2p</sub> XPS spectra of the surface of Mg–Mn, which has been immersed for 216 h in phosphate buffered SBF solution

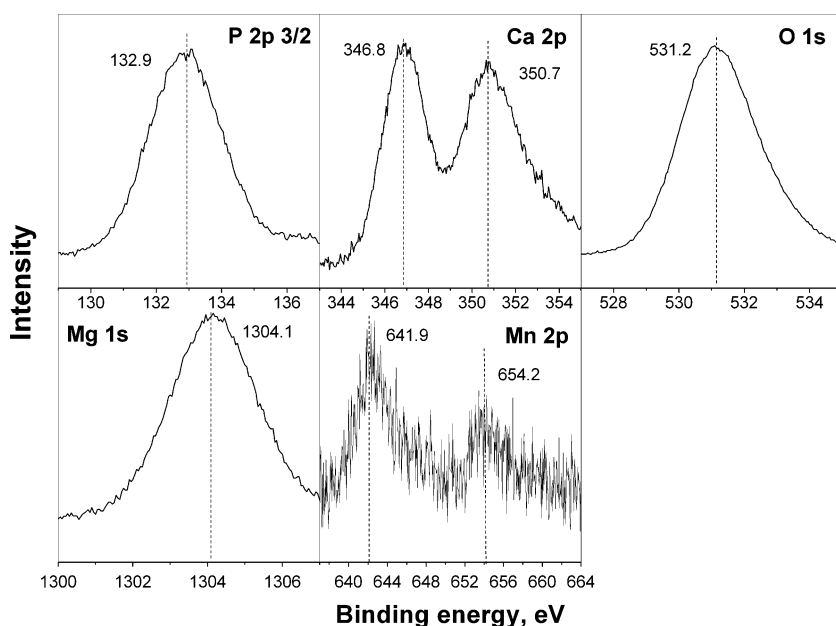


**Fig. 7**  $P_{2p}$ ,  $Ca_{2p}$ ,  $O_{1s}$ ,  $Mg_{1s}$ ,  $Mn_{2p}$  and  $Zn_{2p}$  XPS spectra of the surface of Mg–Mn–Zn, which has been immersed for 216 h in phosphate buffered SBF solution

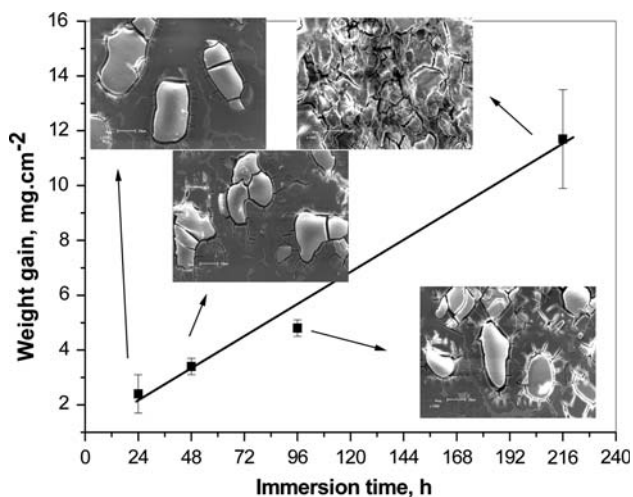
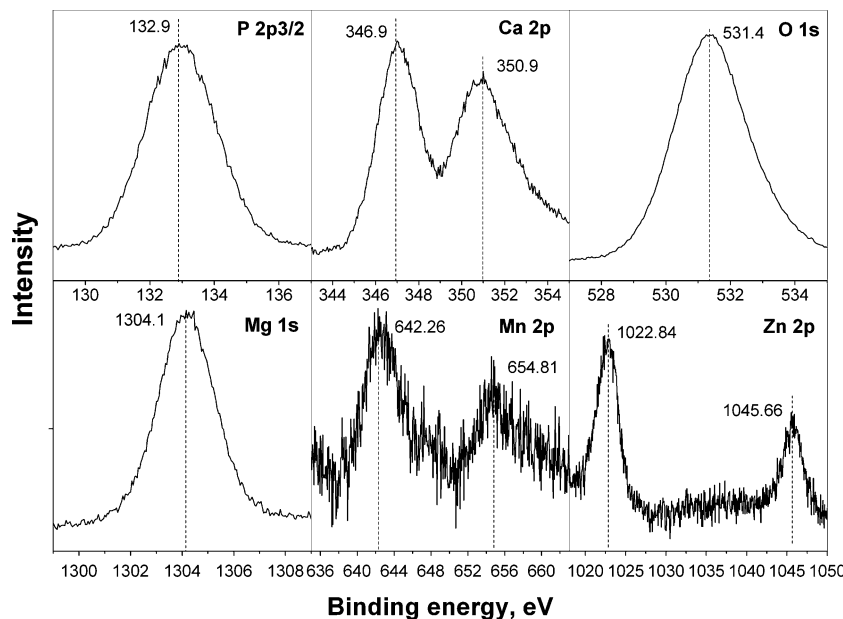


**Fig. 8** Weight gain and morphology of WE43 alloy in the phosphate buffered SBF solution

Figure 10 shows the weight gain rates for Mg–Mn, Mg–Mn–Zn and WE43 alloys. The weight gain rates for all alloys decrease abruptly with the increase of the immersion time within the first 48 h, and then it decreases very slowly or does not change within further immersion. Mg–Mn alloy shows the highest weight gain rate throughout the whole immersion time. The lowest weight gain rate is observed for Mg–Mn–Zn alloy.

Figure 11 shows the weight loss and weight loss rate of three magnesium alloys in phosphate buffered SBF solution. In the weight loss curves, Fig. 11a, the weight loss gradually increases with the increasing of the immersion

time for all alloys. The highest weight loss is observed for Mg–Mn alloy and the lowest weight loss for Mg–Mn–Zn after 216 h immersion. In the weight loss rate curves, Fig. 11b, the weight loss rate of Mg–Mn alloy increase rapidly with immersion time within 24–48 h and decreases rapidly within 48–96 h, and then does not change with immersion time in further immersion. For Mg–Mn–Zn alloy, the weight loss rate increases rapidly within 24–48 h and decreases with immersion time in further immersion. For WE43 alloy, although a similar tendency to that of Mg–Mn alloy is found in the change of the weight loss rate, the change is not significant. For example, only difference of  $0.02 \text{ mg cm}^{-2} \text{ h}^{-1}$  is observed in the weight loss rate between at 24 h and 48 h immersion, indicating that the weight loss rate nearly does not change with immersion within the investigated duration.

## Discussion

The long passivation stage and the noble breakdown potentials obtained from electrochemical measurement for all three alloys demonstrate that a passive layer can be rapidly formed on the magnesium alloy surface, which would provide effective protection to the substrates. Weight gain measurement and the SEM surface microstructure of all alloys clearly confirm that during the immersion a reaction between magnesium alloy and solution happens on the surface. As a result, the alloy surface is covered by a reaction layer for Mg–Mn and Mg–Mn–Zn alloy or product for WE43 alloy. EDS, SAXS and XPS

**Fig. 9** P<sub>2p</sub>, Ca<sub>2p</sub>, O<sub>1s</sub>, Mg<sub>1s</sub> and Y<sub>3d</sub> XPS spectra of the surface of WE43, which has been immersed for 216 h in phosphate buffered SBF solution

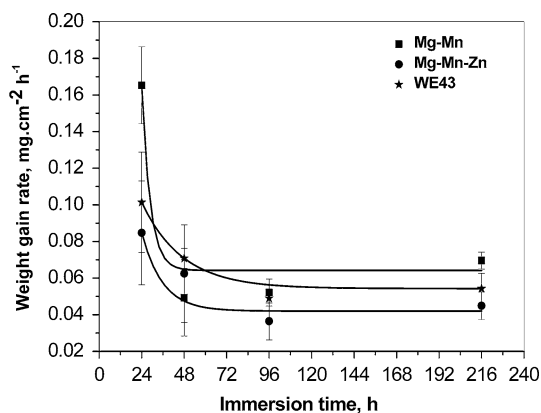
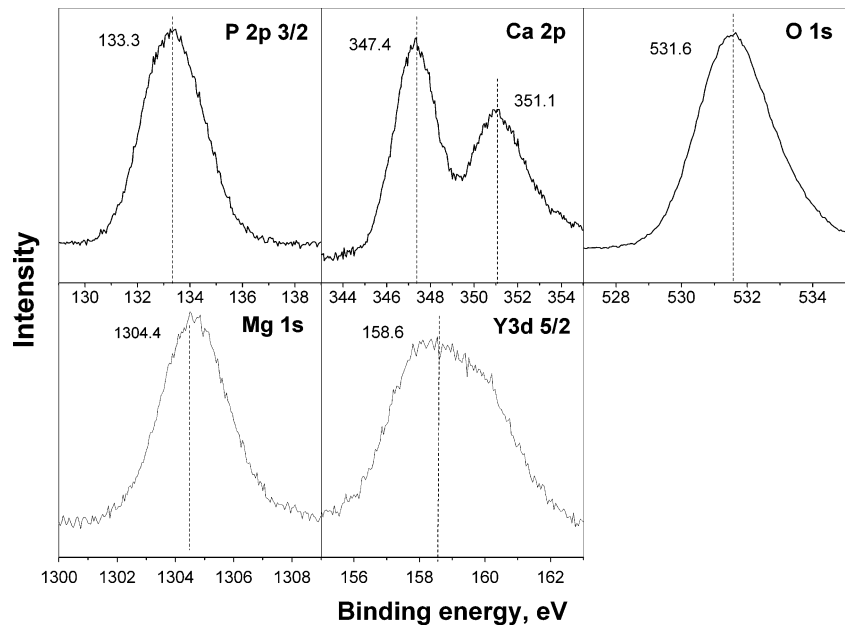


**Fig. 10** Weight gain rates for Mg–Mn, Mg–Mn–Zn and WE43 alloys in phosphate buffered SBF solution

results indicate that the reaction layer or the reaction product is a kind of amorphous Mg containing phosphate, which is mainly composed of O, P, Mg, Na and Ca. In vivo studies have already shown that a calcium phosphate reaction layer was formed around the magnesium implant [1, 20] while relatively high magnesium content was detected in the surrounding bone [20]. Phase identification suggested that the biological calcium phosphate could be formed in this layer [1]. The in vitro corrosion behaviour of magnesium observed in this work is in great agreement with the in vivo results.

From above results, it can be concluded that the corrosion behaviour of magnesium alloys in the phosphate buffered SBF solution happens as following process: dissolving of magnesium in SBF solution by the reaction

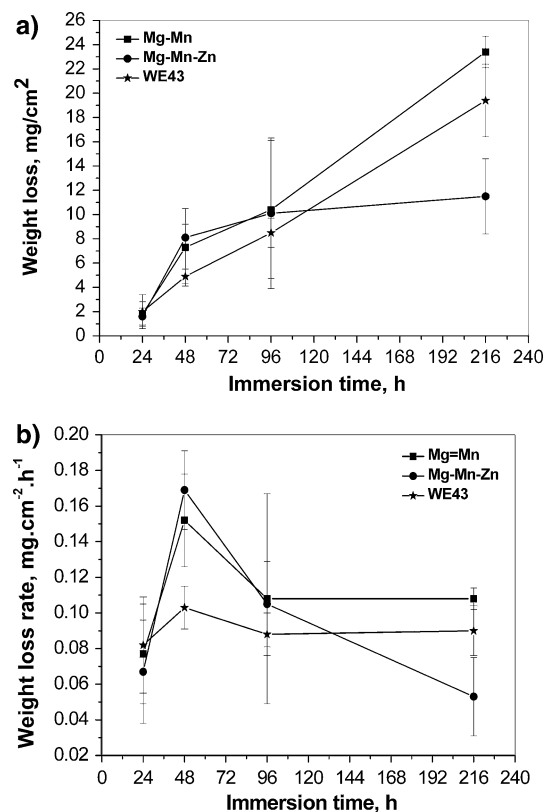


**Fig. 11** Weight loss (a) and weight loss rate (b) of Mg–Mn, Mg–Mn–Zn and WE43 alloys in phosphate buffered SBF solution

between magnesium and solution and precipitating of Mg-containing phosphate layer or product from solution on the surface.

The peak weight loss rate at 48 h in the change of the weight loss rate of Mg–Mn, Mg–Mn–Zn and WE43 against immersion time, Fig. 11b, indicates that weight loss of magnesium alloy through the surface reaction is serious within 96 h, and then the weight loss rate does not change in the further immersion. Meanwhile, the weight gain rate also keeps a constant value after 48–96 h immersion. All these indicate that the weight loss of magnesium through the surface reaction and the weight gain through the precipitation of phosphate reach a stable stage after 48–96 h immersion. Combined with the long passivation stage and the noble breakdown potential in the Fig. 2, it can be summarised that the high activity of magnesium results in the fast reaction between magnesium and phosphate buffered SBF solution, which leads to the fast corrosion of magnesium and fast formation of amorphous Mg-containing phosphate reaction layer on the surface. The formation of this Mg containing phosphate reaction layer could protect magnesium alloy from fast corrosion in the further immersion.

It can be found from the weight loss rate curve that WE43 alloy shows a very good corrosion resistance, especially at the first 48–96 h. After 96 h immersion, the weight loss of Mg–Mn–Zn alloy at 216 h immersion is significantly lower than those of Mg–Mn and WE43 alloys. Meanwhile, a relative high content of Mn and Zn was detected by EDS and XPS in the reaction layer on the surface of Mg–Mn–Zn alloy. Therefore, it can be concluded that this great difference in the weight loss property is mainly due to the difference in surface compositions. Previous studies [21–23] have already proven that the presence of Mn and Zn elements in the Mg alloy and  $\text{Ca}^{2+}$  in the solution could accelerate and promote the formation of the insoluble and protective phosphate layer. The better corrosion resistance of Mg–Mn–Zn alloy suggests that Zn element should be more effective than Mn in the formation of the protective layer in the phosphate buffered solution.

It has been pointed out that pH value of the phosphate buffered solution kept a constant value in a range of 7.3 and 7.4 during the whole immersion test. Therefore, the phosphate buffered solution is not necessary to be refreshed every day due to the increase of pH value as it did in the case of conventional SBF solution or 0.9% NaCl solution. Normally, 0.9% NaCl or Hank's solution is used as the corrosion medium to assess the corrosion property of metals for medical application. The pH value increased rapidly in the case of magnesium alloy to a high value, such as pH = 9 after 1 h immersion and pH = 10 after 3 h [5] and the corrosion rate of magnesium alloy would be inhibited when the pH value is within 10–11[10]. In addition, the reaction product on the magnesium surface is mainly  $\text{Mg}(\text{OH})_2$ , which is quite different from the in vivo research results[1, 20]. From this point of view, the

phosphate buffered solution might be more suitable for the long-term investigation of the corrosion or degradation behaviour of magnesium for biodegradable implant application.

In addition, previous study has pointed out that Mg-containing hydroxyapatite showed a higher osteoconductivity than hydroxyapatite [24]. The Mg-containing phosphate formed on the surface of Mg–Mn and Mg–Mn–Zn suggests that Mg-containing phosphate might contribute to good osteoconductivity of magnesium alloy observed in vivo [1].

## Conclusion

The corrosion behaviour of magnesium alloys in a phosphate buffered SBF solution can be described by the dissolving of magnesium through the reaction between magnesium and solution and the precipitating of Mg-containing phosphate on the surface of magnesium alloy. The addition of Mn and Zn element to magnesium alloy can accelerate the formation of Mg-containing phosphate and in turn provide much better protection for matrix alloy. It is suggested the formation of Mg-containing phosphate on the surface of magnesium might contribute to the good osteoconductivity of magnesium alloy.

**Acknowledgements** One of authors (Erlin Zhang) would like to thank the financial support from Institute of Metal Research and Chinese Academy of Sciences.

## References

1. F. WITTE, V. KAESE, H. HAFERKAMP, E. SWITZER, A. MEYER-LINDENBERG, C. J. WIRTH and H. WINDHAGEN, *Biomaterials* **26** (2005) 3557
2. E. D. MCBRIDE, *J. Am. Med. Assoc.* **111** (1938) 2464
3. V. V. TROITSKII and D. N. TSITRIN, *Khirurgiia* **8** (1944) 41
4. M. S. ZNAMENSKII, *Khirurgiia* **12** (1945) 60
5. H. INOUE, K. SUGAHARA, A. YAMAMOTO and H. TSUBAKINO, *Corrosion Science*, **44** (2002) 603
6. G. L. SONG, A. L. BOWLES and D. H. STJOHN, *Mater. Sci. Eng. A* **A366** (2004) 74–86
7. B. HEUBLEIN, R. ROHDE and V. KAESE, *Heart* **89** (2003) 651
8. H. KUWAHARA, Y. AL-ABDULLAT and M. OHTA, *Mater Sci. Forum* **350–351** (2000) 349
9. H. KUWAHARA, N. MAZAKI, M. MABUCHI, C. WEIN and T. AIZAWAET, *Mater Sci. Forum* **419–422** (2003) 1007
10. D. ZAFFE, C. BERTOLDI and U. Consolo, *Biomaterials* **25** (2004) 3837
11. www.magnesium-elektron.com, Elektron WE43
12. F. WITTE, J. FISCHER, J. NELLESEN, H. CROSTACK, V. KAESE, A. PISCH, F. BECKMANN and H. WINDHAGEN, *Biomaterials*, **27** (2006) 1013
13. <http://www.portfolio.mvm.ed.ac.uk/studentwebs/session2/group29/mangnut.htm>
14. Jef, A. Helsen and H.J. Breme, in “Metals as biomaterials” (Chichester: John Wiley & Sons, 1998) p. 268



15. <http://www.healingwithnutrition.com/mineral.htm> .
16. <http://www.yestonutrition.com/html>.
17. [http://www.merck.com/pubs/mmanual\\_home/sec12/135.htm](http://www.merck.com/pubs/mmanual_home/sec12/135.htm)
18. <http://www.nutrition.org/nutinfo/>
19. M. M. Avedesian and H. Baker, in “ASM specialty handbook, Magnesium and magnesium alloys” (The Materials Information Society, 1990), p. 15
20. G. N. Yu, E. L. Zhang, L. P. Xu and K. Yang, in “2006 Beijing International Materials Week”, June 25–30, Beijing, China, p. 331
21. K. Z. CHONG and T. S. SHIH, *Mater. Chem. Phys.* **80** (2003) 191
22. G. LORIN. in Phosphating of metals (Middlesex: Finishing publications LTD, 1974), p. 32
23. L. KOUISNI, M. AZZI, M. ZERTOUBI, F. DALARD and S. MAXIMOVITCH, *Surf. Coat. Tech.* **185** (2004) 58
24. S. R. KIM, J. H. LEE, Y. T. KIM, D. H. RIU, S. J. JUNG, Y. J. LEE, S. C. CHUNG and Y. H. KIM, *Biomaterials* **24** (2003) 1389